Diffusion-weighted Magnetic Resonance Imaging in Odontogenic Keratocysts: Preliminary Study on Usefulness of Apparent Diffusion Coefficient Maps for Characterization of Normal Structures and Lesions

Ichiro OGURA[1], Ken NAKAHARA[2], Yoshihiko SASAKI[1], Mikiko SUE[1], Takaaki ODA[1]

Objective: *To investigate the usefulness of diffusion-weighted magnetic resonance imaging (DWI) in odontogenic keratocysts, especially apparent diffusion coefficient (ADC) maps for the characterisation of normal structures and cystic lesions in the jaw.*
Methods: *Sixteen patients who underwent magnetic resonance imaging (MRI) for the diagnosis of a cystic lesion in the jaw were included in this prospective study. DWI was performed on a 1.5 T unit with b factor of 0 and 800 s/mm^2, and ADC maps were generated. ADC values were measured for the normal structures in the upper neck area and for the cystic lesion in the jaw.*
Results: *The mean ADC value of the cerebrospinal fluid ($3.66 \pm 0.47 \times 10^{-3}$ mm^2/s) in the upper neck area was higher than that of the nasal mucosa ($1.80 \pm 0.19 \times 10^{-3}$ mm^2/s), Waldeyer's ring ($0.75 \pm 0.11 \times 10^{-3}$ mm^2/s) and the spinal cord ($0.71 \pm 0.20 \times 10^{-3}$ mm^2/s). The mean ADC value of the five odontogenic keratocysts ($1.03 \pm 0.31 \times 10^{-3}$ mm^2/s) was lower than that of the one simple bone cyst (2.79×10^{-3} mm^2/s), three nasopalatine duct cysts ($2.28 \pm 0.12 \times 10^{-3}$ mm^2/s), three radicular cysts ($1.82 \pm 0.71 \times 10^{-3}$ mm^2/s) and four dentigerous cysts ($1.67 \pm 1.06 \times 10^{-3}$ mm^2/s).*
Conclusion: *This study suggested the usefulness of DWI in odontogenic keratocysts, especially ADC maps for the characterization of normal structures and cystic lesions in the jaw.*
Key words: *magnetic resonance imaging (MRI), diffusion, cyst, odontogenic*
Chin J Dent Res 2019;22(1):51–56; doi: 10.3290/j.cjdr.a41775

The 4th edition of the World Health Organization's Classification of Head and Neck Tumours was published in January 2017[1,2]. The most controversial decision in the 2017 classification was to move keratocystic odontogenic tumour back into the cyst category as odontogenic keratocyst. The evidence for reclassification was based on "aggressive growth", recurrence after treatment and the rare occurrence of a "solid" variant of an odontogenic keratocyst.

1 Radiology, The Nippon Dental University Niigata Hospital, Niigata, Japan.
2 Advanced Research Center, The Nippon Dental University School of Life Dentistry at Niigata, Niigata, Japan.

Corresponding author: Dr Ichiro OGURA, Radiology, The Nippon Dental University Niigata Hospital, 1-8 Hamaura-cho, Chuo-ku, Niigata, Niigata 951-8580, Japan. Tel: 81 25 267 1500; Fax: 81 25 267 1134. Email: ogura@ngt.ndu.ac.jp

Diagnosis of head and neck lesions is difficult due to the complicated anatomic structure and different histological components of the many tissues of the neck[3]. Imaging oral and maxillofacial lesions is not only important for the diagnosis of lesions, but also for the differentiation of benign lesions from malignant lesions and the staging of tumours. Conventional imaging methods such as computed tomography (CT) and magnetic resonance imaging (MRI) mainly evaluate morphological properties; their value is limited in recognizing prognostic characteristics such as the benign–malignant differentiation of lesions[4].

Diffusion-weighted MRI (DWI) is a short sequence produced from echo-planar imaging (EPI) and fast advanced spin echo (FASE) sequences[5]. DWI with apparent diffusion coefficient (ADC) maps, which provides a quantitative index of water diffusivity for each voxel that allows the visualisation of the microscopic

motion of water molecules within tissues, can facilitate data acquisition and processing steps without the use of ionising radiation or contrast agents[6]. Therefore, in recent years, DWI has been considered a good candidate as a non-invasive biomarker for predicting and monitoring treatment responses. Furthermore, some studies have reported the application of DWI with the calculation of ADC in the differentiation between benign and malignant head and neck masses[7-11].

Based on DWI studies, ADC maps were proposed to be useful for differentiating between keratocystic odontogenic tumours and ameloblastomas, whereas they contributed little to differentiating keratocystic odontogenic tumours from odontogenic cysts such as radicular cysts and dentigerous cysts[12-15]. However, to the best of the authors' knowledge, DWI in odontogenic cysts, especially the usefulness of ADC maps for the characterization of normal structures and cystic lesions in the jaw, have been little reported in the literature. The aim of this study was to investigate the usefulness of DWI in odontogenic cysts, especially ADC maps for the characterization of normal structures in the upper neck area and cystic lesions in the jaw.

Materials and methods

Patients

This prospective study was approved by the ethics committee of our institution. After providing written informed consent, 16 patients (10 male, 6 female; age 25 to 85 years, mean age 50.6 years) with cystic lesions in the jaw underwent MRI at our university hospital from October 2016 to February 2018. This study included five odontogenic keratocysts (one in the maxilla, four in the mandible), three nasopalatine duct cysts (all in the maxilla), three radicular cysts (one in the maxilla, two in the mandible), four dentigerous cysts (one in the maxilla, three in the mandible) and one simple bone cyst (in the mandible). The histopathological diagnoses of these lesions were obtained by surgery in all cases after MRI.

MRI techniques

The MR images (1.5 Tesla MR unit; EXCELART Vantage MRT-2003; Canon Medical Systems, Otawara, Japan) with a head coil included unenhanced axial T1-weighted imaging (T1WI; repetition time [TR] 660 ms, echo time [TE] 12 ms), T2-weighted imaging (T2WI; TR 4000 ms, TE 120 ms), and short TI inversion recovery sequences (STIR) (TR 2500 ms, TE 15 ms, TI 190 ms). An isotropic DWI sequence was obtained with b values of 0 and 800 s/mm^2 with an EPI technique. The following technical parameters were used: TR 8476 ms, TE 80 ms. The ADC maps and maximum intensity projection (MIP) were automatically calculated from the DWI with b = 800 s/mm^2.

Data analysis

Two oral and maxillofacial radiologists with over 20 years of experience independently reviewed all the images and any discrepancies were resolved by consensus. The MR images of the lesions were assessed with special attention to intensity changes. A region of interest (ROI) was used to calculate the ADC values on ADC maps. Three ROIs with similar sizes within the lesions were measured to obtain a mean ADC value. The mean of two observers' evaluations of the ADC value was used as each lesion's representative value. We also measured the ADC value of Waldeyer's ring, the nasal mucosa, the spinal cord, and the cerebrospinal fluid in the upper neck area as normal structures.

Statistical analysis

Interobserver agreement was evaluated using the interclass correlation coefficient (ICC). Interobserver agreement was considered excellent for ICC > 0.75; in case of ICC ≥ 0.40 but ≤ 0.75 the agreement was considered fair to good; an ICC < 0.40 was regarded as poor.

The statistical analysis among the ADC values of normal structures in the upper neck area was performed using one-way repeated measures analysis of variance (ANOVA). The ADC values of the odontogenic keratocysts and the other cysts were evaluated by the Mann-Whitney U test. These analyses were performed with the statistical package IBM SPSS Statistics version 24 (IBM Japan, Tokyo, Japan). A P value of < 0.05 was considered statistically significant.

Results

The ICC of the ADC values was 0.999 (P = 0.000). The interobserver agreement was considered excellent for the ADC values. Table 1 shows the imaging features of cystic lesions in the jaw using MRI. Regarding odontogenic keratocysts, the T1-weighted image shows a low signal intensity area (Fig 1a). The T2-weighted image and STIR show a high signal intensity area (Fig 1b and c). The diffusion-weighted image shows a high signal intensity area (Fig 1d). The ADC map shows a low

Table 1 Imaging features of cystic lesion in the jaw with MRI.

Case	Age (years)	Gender	Location	Lesion	MRI findings						
					Internal signal	T1WI	T2WI	STIR	DWI	ADC map	ADC value ($\times 10^{-3}$ mm^2/s)
1	70	Female	Mandible	Simple bone cyst	Homogeneous	Low	High	High	High	High	2.79
2	74	Female	Mandible	Radicular cyst	Homogeneous	Low	High	High	High	High	2.63
3	32	Male	Mandible	Dentigerous cyst	Homogeneous	Low	High	High	High	High	2.63
4	74	Male	Maxilla	Dentigerous cyst	Heterogeneous	High	High	High	High	High	2.52
5	41	Male	Maxilla	Nasopalatine duct cyst	Heterogeneous	High	High	High	High	High	2.42
6	72	Male	Maxilla	Nasopalatine duct cyst	Heterogeneous	High	High	High	High	High	2.25
7	70	Female	Maxilla	Nasopalatine duct cyst	Heterogeneous	Low	High	High	High	High	2.18
8	40	Male	Maxilla	Radicular cyst	Homogeneous	Low	High	High	High	Low	1.50
9	35	Female	Mandible	Odontogenic keratocyst	Heterogeneous	Low	High	High	High	Low	1.49
10	41	Male	Mandible	Radicular cyst	Homogeneous	Low	High	High	High	Low	1.33
11	38	Male	Mandible	Odontogenic keratocyst	Heterogeneous	Low	High	High	High	Low	1.09
12	85	Female	Maxilla	Odontogenic keratocyst	Heterogeneous	Low	High	High	High	Low	1.08
13	62	Male	Mandible	Dentigerous cyst	Heterogeneous	High	High	Low	High	Low	0.97
14	25	Female	Mandible	Odontogenic keratocyst	Heterogeneous	Low	High	High	High	Low	0.77
15	25	Male	Mandible	Odontogenic keratocyst	Heterogeneous	Low	High	High	High	Low	0.71
16	26	Male	Mandible	Dentigerous cyst	Homogeneous	High	High	High	High	Low	0.55

MRI: magnetic resonance imaging, T1WI: T1-weighted image, T2WI: T2-weighted image, STIR: short TI inversion recovery image, DWI: diffusion-weighted image, ADC: apparent diffusion coefficient.

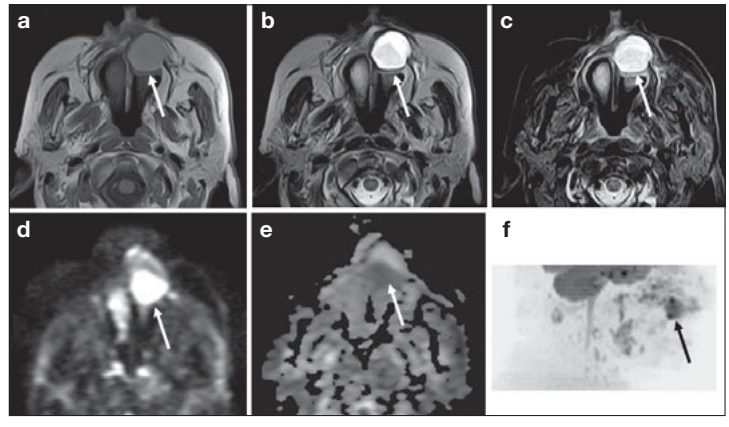

Fig 1 Odontogenic keratocyst of the maxilla in an 85-year-old female. **(a)** The T1-weighted image shows a low signal intensity area (arrow). **(b and c)** The T2-weighted image and STIR show a high signal intensity area (arrow). **(d)** The diffusion-weighted image shows a high signal intensity area (arrow). **(e)** The ADC map shows a low signal intensity area (arrow). **(f)** The MIP (DWI) shows lesions in an improved way (arrow).

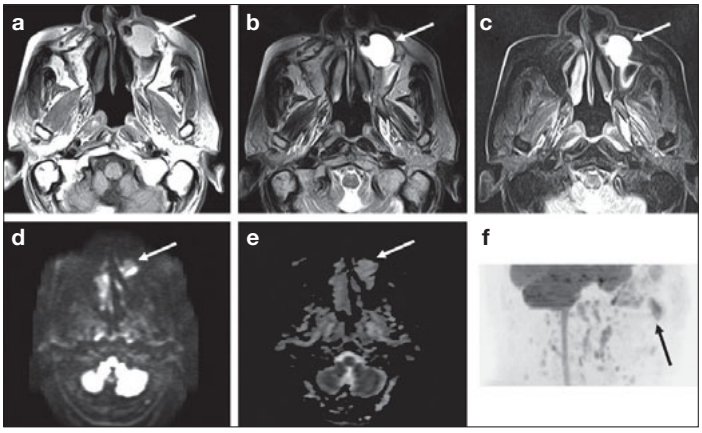

Fig 2 Dentigerous cyst of the maxilla in a 74-year-old male. **(a)** The T1-weighted image shows a high signal intensity area (arrow). **(b and c)** The T2-weighted image and STIR show a high signal intensity area (arrow). **(d)** The diffusion-weighted image shows a high signal intensity area (arrow). **(e)** The ADC map shows a high signal intensity area (arrow). **(f)** The MIP (DWI) shows lesions in an improved way (arrow).

signal intensity area (Fig 1e). The MIP (DWI) shows lesions in an improved way (Fig 1f). Regarding the dentigerous cyst, the T1-weighted image shows a high signal intensity area (Fig 2a). The T2-weighted image and STIR show a high signal intensity area (Fig 2b and c). The diffusion-weighted image shows a high signal intensity area (Fig 2d). The ADC map shows a high signal intensity area (Fig 2e). The MIP (DWI) shows lesions in an improved way (Fig 2f).

Table 2 shows the ADC values of normal structures in the upper neck area and cystic lesions in the jaw. Regarding the normal structures, the mean ADC value of the cerebrospinal fluid ($3.66 \pm 0.47 \times 10^{-3}$ mm^2/s) in the upper neck area was significantly higher than that of the nasal mucosa ($1.80 \pm 0.19 \times 10^{-3}$ mm^2/s), Waldeyer's ring ($0.75 \pm 0.11 \times 10^{-3}$ mm^2/s) and the spinal cord ($0.71 \pm 0.20 \times 10^{-3}$ mm^2/s) ($P = 0.000$). Regarding cystic lesions, the mean ADC value of odontogenic keratocysts ($1.03 \pm 0.31 \times 10^{-3}$ mm^2/s) was lower than that of simple bone cysts (2.79×10^{-3} mm^2/s), nasopalatine duct cysts ($2.28 \pm 0.12 \times 10^{-3}$ mm^2/s), radicular cysts ($1.82 \pm 0.71 \times 10^{-3}$ mm^2/s) and dentigerous cysts ($1.67 \pm 1.06 \times 10^{-3}$ mm^2/s). Furthermore, the mean ADC value of odontogenic keratocysts was significantly lower than that of the other cysts in the jaw ($1.98 \pm 0.76 \times 10^{-3}$ mm^2/s; $P = 0.038$).

Discussion

Helenius et al[16] showed that ADC values in the normal human brain were highest in the cortical grey matter ($0.89 \pm 0.04 \times 10^{-3}$ mm^2/s), lower in the deep grey matter ($0.75 \pm 0.03 \times 10^{-3}$ mm^2/s) and lowest in the white matter ($0.70 \pm 0.03 \times 10^{-3}$ mm^2/s). In this study, regarding normal structures in 16 patients, the mean ADC value of the cerebrospinal fluid ($3.66 \pm 0.47 \times 10^{-3}$ mm^2/s) in the upper neck area was higher than that of the nasal mucosa ($1.80 \pm 0.19 \times 10^{-3}$ mm^2/s), Waldeyer's ring ($0.75 \pm 0.11 \times 10^{-3}$ mm^2/s) and the spinal cord ($0.71 \pm 0.20 \times 10^{-3}$ mm^2/s). We consider that the evaluation of ADC values in the normal structures is important for differential diagnosis of oral and maxillofacial lesions.

The ADC values of malignant lesions have been found to be lower than that of benign lesions by a significant amount in head and neck studies[4]. Şerifoğlu et al[3] indicated that the median ADC value of malignant tumours and benign lesions were 0.72×10^{-3} mm^2/s and 1.17×10^{-3} mm^2/s, respectively ($P < 0.001$). Sakamoto et al[8] showed that the mean ADC value of cysts was $2.41 \pm 0.48 \times 10^{-3}$ mm^2/s, which was significantly higher than that of benign ($1.48 \pm 0.62 \times 10^{-3}$ mm^2/s) and malignant ($1.23 \pm 0.45 \times 10^{-3}$ mm^2/s) tumours ($P < 0.001$). Srinivasan et al[17] showed that there was a statistically significant difference ($P = 0.004$) between the mean ADC values in benign ($1.505 \pm 0.487 \times 10^{-3}$ mm^2/s) and malignant ($1.071 \pm 0.293 \times 10^{-3}$ mm^2/s) lesions in the head and neck. Abdel Razek et al[9] showed that the mean ADC values of malignant tumours, benign solid masses and cystic lesions were $0.93 \pm 0.18 \times 10^{-3}$ mm^2/s, $1.57 \pm 0.26 \times 10^{-3}$ mm^2/s and $2.01 \pm 0.21 \times 10^{-3}$ mm^2/s, respectively. Furthermore, Maeda et al[18] showed that mean ADC values were $0.96 \pm 0.11 \times 10^{-3}$ mm^2/s for SCC and $0.65 \pm 0.09 \times 10^{-3}$ mm^2/s for lymphoma in the head and neck; the difference was significant ($P < 0.001$).

Based on DWI studies, the ADC was proposed to be useful for differentiating keratocystic odontogenic tumours from ameloblastomas, whereas the ADC contributed little to differentiating keratocystic odontogenic tumours from odontogenic cysts such as radicular cysts

Table 2 ADC values of normal structures in the upper neck area and cystic lesions in the jaw.

	Number	ADC (× 10^{-3} mm^2s^{-1})	
		Mean ± SD (Range)	*P* value
Normal structures in the upper neck area			0.000
Spinal cord	16	0.71 ± 0.20 (0.36 - 0.97)	
Waldeyer's ring	16	0.75 ± 0.11 (0.60 - 0.98)	
Nasal mucosa	16	1.80 ± 0.19 (1.40 - 2.20)	
Cerebrospinal fluid	16	3.66 ± 0.47 (2.73 - 4.35)	
Cystic lesions in the jaw			0.038
Odontogenic keratocyst	5	1.03 ± 0.31 (0.71 - 1.49)	
Other cysts	11	1.98 ± 0.76 (0.55 - 2.79)	
Simple bone cyst	1	2.79	
Nasopalatine duct cyst	3	2.28 ± 0.12 (2.18 - 2.42)	
Radicular cyst	3	1.82 ± 0.71 (1.33 - 2.63)	
Dentigerous cyst	4	1.67 ± 1.06 (0.55 - 2.63)	

ADC: apparent diffusion coefficient, SD: standard deviation.

and dentigerous cysts[12-15]. Sumi et al[12] showed that the mean ADC values of non-enhancing lesions in ameloblastomas, non-enhancing lesions in keratocystic odontogenic tumours and solid lesions in ameloblastomas were 2.48 ± 0.20 × 10^{-3} mm^2/s, 1.13 ± 0.56 × 10^{-3} mm^2/s and 1.39 ± 0.15 × 10^{-3} mm^2/s, respectively. Srinivasan et al[13] showed that the mean ADC values of the cystic areas of ameloblastomas and the solid areas of both ameloblastomas and keratocystic odontogenic tumours were 2.192 ± 0.33 × 10^{-3} mm^2/s, 1.041 ± 0.41 × 10^{-3} mm^2/s and 1.019 ± 0.07 × 10^{-3} mm^2/s, respectively. Eida et al[14] showed that the mean ADC values of the fluid areas of ameloblastomas, simple bone cysts, dentigerous cysts, radicular cysts and keratocystic odontogenic tumours were 2.45 ± 0.27 × 10^{-3} mm^2/s, 2.52 ± 0.14 × 10^{-3} mm^2/s, 1.50 ± 0.49 × 10^{-3} mm^2/s, 0.90 ± 0.21 × 10^{-3} mm^2/s and 0.87 ± 0.13 × 10^{-3} mm^2/s, respectively. However, these reports were relatively short. Moreover, several types of cysts and tumours can occur in the oral and maxillofacial region. Therefore, further study is necessary to validate these results.

In the present study, the mean ADC value of odontogenic keratocysts (1.03 ± 0.31 × 10^{-3} mm^2/s) was lower than that of simple bone cysts (2.79 × 10^{-3} mm^2/s), nasopalatine duct cysts (2.28 ± 0.12 × 10^{-3} mm^2/s), radicular cysts (1.82 ± 0.71 × 10^{-3} mm^2/s) and dentigerous cysts (1.67 ± 1.06 × 10^{-3} mm^2/s). Driessen et al[4] indicated that DWI showed consistently high accuracy and high negative predictive values in head and neck squamous cell carcinomas. Bonello et al[19] showed that DWI is a non-invasive imaging tool potentially able to provide information about microstructural tumour characteristics. In this study, the mean ADC value of odontogenic keratocysts (1.03 ± 0.31 × 10^{-3} mm^2/s) was significantly lower than that of the other cysts in the jaw (1.98 ± 0.76 × 10^{-3} mm^2/s; $\beta = 0.038$). We consider that ADC values of lesions are linked to the histopathological differences between tumours and cystic lesions.

In conclusion, this study suggested the usefulness of DWI in odontogenic keratocysts, especially ADC maps for the characterization of normal structures and cystic lesions in the jaw.

Conflicts of interest

The authors reported no conflicts of interest related to this study.

Author contribution

Dr Ichiro OGURA designed the study, acquired the case data and prepared the manuscript; Dr Ken NAKAHARA approved the final revised manuscript; Dr Yoshihiko SASAKI revised the manuscript; Dr Mikiko SUE analysed the radiological data; Dr Takaaki ODA interpreted the radiological data.

(Received Dec 12, 2017; accepted March 8, 2018)

References

1. Wright JM, Vered M. Update from the 4th Edition of the World Health Organization Classification of Head and Neck Tumours: Odontogenic and Maxillofacial Bone Tumors. Head Neck Pathol 2017;11:68–77.
2. Speight PM, Takata T. New tumour entities in the 4th edition of the World Health Organization Classification of Head and Neck tumours: odontogenic and maxillofacial bone tumours. Virchows Arch 2018;472:331–339.
3. Şerifoğlu İ, Oz İİ, Damar M, Tokgöz Ö, Yazgan Ö, Erdem Z. Diffusion-weighted imaging in the head and neck region: usefulness of apparent diffusion coefficient values for characterization of lesions. Diagn Interv Radiol 2015;21:208–214.
4. Driessen JP, van Kempen PM, van der Heijden GJ, et al. Diffusion-weighted imaging in head and neck squamous cell carcinomas: a systematic review. Head Neck 2015;37:440–448.
5. Sakamoto J, Sasaki Y, Otonari-Yamamoto M, Sano T. Comparison of various methods for quantification of apparent diffusion coefficient of head and neck lesions with HASTE diffusion-weighted MR imaging. Oral Surg Oral Med Oral Pathol Oral Radiol 2012;114:266–276.
6. Ryoo I, Kim JH, Choi SH, Sohn CH, Kim SC. Squamous cell carcinoma of the head and neck: comparison of diffusion-weighted MRI at b-values of 1,000 and 2,000 s/mm2 to predict response to induction chemotherapy. Magn Reson Med Sci 2015;14:337–345.
7. Li S, Cheng J, Zhang Y, Zhang Z. Differentiation of benign and malignant lesions of the tongue by using diffusion-weighted MRI at 3.0T. Dentomaxillofac Radiol 2015;44:20140325.
8. Sakamoto J, Yoshino N, Okochi K, et al. Tissue characterization of head and neck lesions using diffusion-weighted MR imaging with SPLICE. Eur J Radiol 2009;69:260–268.
9. Abdel Razek AA, Gaballa G, Elhawarey G, Megahed AS, Hafez M, Nada N. Characterization of pediatric head and neck masses with diffusion-weighted MR imaging. Eur Radiol 2009;19:201–208.
10. Schakel T, Hoogduin JM, Terhaard CH, Philippens ME. Diffusion weighted MRI in head-and-neck cancer: geometrical accuracy. Radiother Oncol 2013;109:394–397.
11. Kato H, Fujimoto K, Matsuo M, Mizuta K, Aoki M. Usefulness of diffusion-weighted MR imaging for differentiating between Warthin's tumor and oncocytoma of the parotid gland. Jpn J Radiol 2017;35:78–85.
12. Sumi M, Ichikawa Y, Katayama I, Tashiro S, Nakamura T. Diffusion-weighted MR imaging of ameloblastomas and keratocystic odontogenic tumors: differentiation by apparent diffusion coefficients of cystic lesions. AJNR Am J Neuroradiol 2008;29:1897–1901.
13. Srinivasan K, Seith Bhalla A, Sharma R, Kumar A, Roychoudhury A, Bhutia O. Diffusion-weighted imaging in the evaluation of odontogenic cysts and tumours. Br J Radiol 2012;85:e864–e870.
14. Eida S, Hotokezaka Y, Katayama I, et al. Apparent diffusion coefficient-based differentiation of cystic lesions of the mandible. Oral Radiol 2012;28:109–114.
15. Sakamoto J, Kuribayashi A, Kotaki S, Fujikura M, Nakamura S, Kurabayashi T. Application of diffusion kurtosis imaging to odontogenic lesions: Analysis of the cystic component. J Magn Reson Imaging 2016;44:1565–1571.
16. Helenius J, Soinne L, Perkiö J, et al. Diffusion-weighted MR imaging in normal human brains in various age groups. AJNR Am J Neuroradiol 2002;23:194–199.
17. Srinivasan A, Dvorak R, Perni K, Rohrer S, Mukherji SK. Differentiation of benign and malignant pathology in the head and neck using 3T apparent diffusion coefficient values: early experience. AJNR Am J Neuroradiol 2008;29:40–44.
18. Maeda M, Kato H, Sakuma H, Maier SE, Takeda K. Usefulness of the apparent diffusion coefficient in line scan diffusion-weighted imaging for distinguishing between squamous cell carcinomas and malignant lymphomas of the head and neck. AJNR Am J Neuroradiol 2005;26:1186–1192.
19. Bonello L, Preda L, Conte G, et al. Squamous cell carcinoma of the oral cavity and oropharynx: what does the apparent diffusion coefficient tell us about its histology? Acta Radiol 2016;57:1344–1351.